




Interstitial-Induced Ferromagnetism in a Two-Dimensional Wigner Crystal

Kyung-Su Kim (김경수) ^{*}, Chaitanya Murthy , Akshat Pandey , and Steven A. Kivelson 
Department of Physics, Stanford University, Stanford, California 93405, USA

 (Received 9 July 2022; accepted 27 October 2022; published 22 November 2022)

The two-dimensional Wigner crystal (WC) occurs in the strongly interacting regime ($r_s \gg 1$) of the two-dimensional electron gas (2DEG). The magnetism of a pure WC is determined by tunneling processes that induce multispin ring-exchange interactions, resulting in fully polarized ferromagnetism for large enough r_s . Recently, Hossain *et al.* [*Proc. Natl. Acad. Sci. U.S.A.* **117**, 32244 (2020)] reported the occurrence of a fully polarized ferromagnetic insulator at $r_s \gtrsim 35$ in an AIAs quantum well, but at temperatures orders of magnitude larger than the predicted exchange energies for the pure WC. Here, we analyze the large r_s dynamics of an interstitial defect in the WC, and show that it produces local ferromagnetism with much higher energy scales. Three hopping processes are dominant, which favor a large, fully polarized ferromagnetic polaron. Based on the above results, we speculate concerning the phenomenology of the magnetism near the metal-insulator transition of the 2DEG.

DOI: [10.1103/PhysRevLett.129.227202](https://doi.org/10.1103/PhysRevLett.129.227202)

The two-dimensional electron gas (2DEG) has proven to be a rich platform for studying strongly correlated phases of matter, despite its deceptively simple Hamiltonian

$$H = \sum_i \frac{\vec{p}_i^2}{2m} + \sum_{i < j} \frac{e^2}{4\pi\epsilon |\vec{r}_i - \vec{r}_j|}. \quad (1)$$

The important dimensionless parameter in the problem is the ratio r_s of the typical interaction and kinetic energies; $r_s = 1/(a_B \sqrt{\pi n})$, where n is the electron density and $a_B = 4\pi\epsilon\hbar^2/me^2$ is the effective Bohr radius. The electrons form an unpolarized Fermi liquid (FL) when r_s is small, whereas a Wigner crystal (WC) phase occurs when $r_s > r_{wc} \approx 31 \pm 1$ [1–4]. Recently, experiments on “ultra-clean” AIAs quantum wells reported the appearance of a fully polarized ferromagnetic insulating phase when $r_s \gtrsim 35$ [5–7], where the WC physics may play a key role. Ferromagnetic tendencies near the metal-insulator transition have also been seen in a variety of other 2DEG systems [8,9]. In this paper we explore a new mechanism of ferromagnetism in the large- r_s regime.

There have been many previous theoretical studies of the magnetism of the WC [10–14]. Deep within the WC phase (in the $r_s \rightarrow \infty$ limit), a semiclassical instanton method allows an asymptotically exact calculation of various multispin ring exchange energies J_{wc} . The result of these calculations is that the WC (and hence the 2DEG) is fully spin polarized in the $r_s \rightarrow \infty$ limit [10–12]. This result has been corroborated by a path integral Monte Carlo calculation [13]. Therefore it is tempting to say that the observed fully polarized ferromagnetic insulator is the ferromagnetic WC. However, we will see that such a mechanism provides a minuscule energy scale (i.e., temperature scale T^*) for the

ferromagnetism, which is much below those accessed in the experiments. Moreover, the theoretical studies suggest [10–14] that the dominant exchange interactions are actually antiferromagnetic in the experimentally relevant range of $r_s \sim 40$ of the 2DEG.

We instead propose a new mechanism for ferromagnetism at large r_s , induced by interstitial defects centered at triangular plaquettes of the WC [15–17]. (This idea was inspired by a related, but distinct, earlier proposal by Spivak and collaborators [18,19] of ferromagnetism produced by interfacial fluctuations between a WC and a FL.) The presence of interstitials generates additional exchange (J_a) and hopping (t_a) processes, which we calculate using the semiclassical instanton method. See Fig. 1 for a summary of the results. Three hopping processes turn out to have (exponentially) large energy scales compared to any exchange energy of the defect-free WC. We prove that a single interstitial fully polarizes a large region of the WC (i.e., produces a large ferromagnetic polaron), and argue that a dilute concentration of interstitials will lead to a fully polarized ferromagnetic ground state. Moreover, the characteristic temperature scale of the ferromagnet is $T^* \sim \nu_{int} \cdot t$, where $0 \leq \nu_{int} \leq 1$ is the filling of interstitial sites and t is an appropriate sum of hopping energies t_a . At the values of r_s pertinent to the experiments, T^* is in the experimentally relevant range, even for a low concentration of interstitials.

In order to discuss the possible experimental relevance of these results, we must consider circumstances that can give rise to a finite density of interstitials. On the phenomenological level, near the metal-insulator transition, it is likely that the 2DEG sample forms a spatially inhomogeneous mixture of regions that exhibit local WC order (with lower

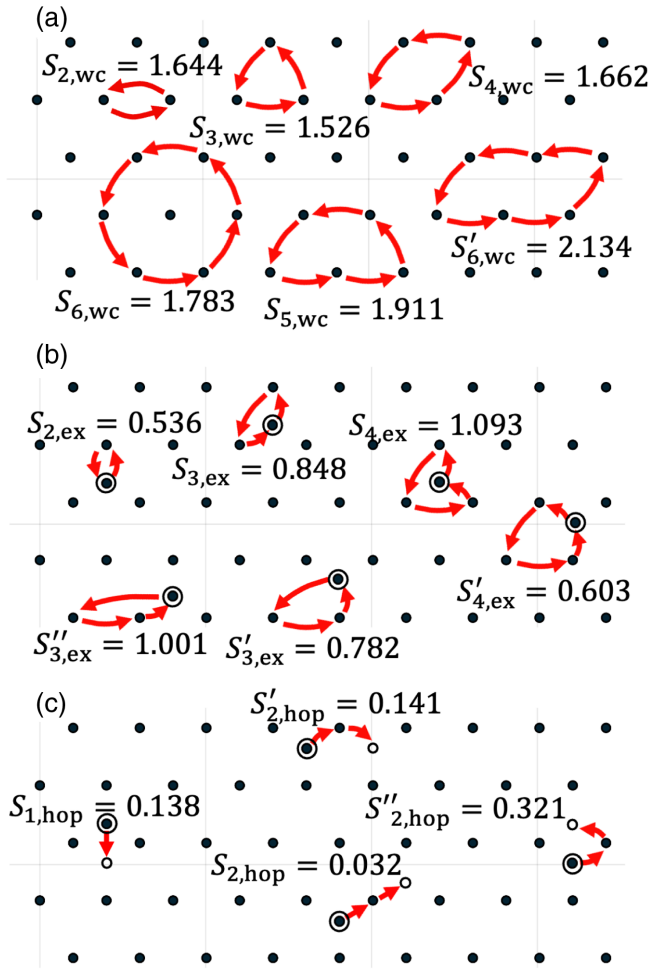


FIG. 1. Schematic of various exchange and hopping processes along with the corresponding dimensionless actions S_a : (a) Exchange processes in the pure WC. (b) New exchange processes in the WC induced by a triangle-centered interstitial. (c) Hopping processes in the WC induced by the interstitial. In panels (b) and (c), dots surrounded by a circle denote initially occupied interstitial sites, while open circles denote final interstitial sites which are initially vacant. The dimensionless actions in panel (a) are quoted from Ref. [14]. Panels (b) and (c) show the main results of this paper, calculated with a system of size $10 \times 12 + 1$ starting from the *relaxed* triangle-centered interstitial configuration (see the main text and the Supplemental Material [20] for details). The corresponding values for the exchange couplings, J_a , and the hopping matrix elements, t_a , are then computed using Eq. (3) and its analog.

than average electron density) coexisting with puddles of FL (with higher density). This can arise as a consequence of disorder [21,22] and/or could reflect the electronic microemulsion phases expected when macroscopic phase separation is frustrated by long-range interactions [23–26]. Consequently, a finite density of extra electrons would be induced at the boundaries of WC regions due to their contact with higher-density FL regions. The lowest energy WC defect that can accommodate an extra electron is known to be the triangle-centered interstitial [15–17].

Semiclassical derivation of the effective Hamiltonian.— For orientation, we start by recapitulating the semiclassical theory of magnetism in the WC. In the $r_s \rightarrow \infty$ limit, the Coulomb interaction dominates, and the electrons form a WC [1] with all spin states degenerate. The kinetic energy lifts this degeneracy by inducing quantum tunneling processes among WC sites. The effective spin Hamiltonian can be written as a sum over ring exchange terms:

$$H_{\text{eff}}^{\text{WC}} = \sum_a (-1)^{n_a} J_a (\hat{P}_a + \hat{P}_a^{-1}). \quad (2)$$

Here, $a = (i_1, i_2, \dots, i_{n_a})$ labels a ring exchange process involving n_a sites, $i_1 \rightarrow i_2 \rightarrow \dots \rightarrow i_{n_a} \rightarrow i_1$, and \hat{P}_a is the corresponding n_a -particle cyclic permutation operator. \hat{P}_a can, in turn, be expressed as a product of two-particle exchange operators, each of which can be written in terms of spin operators as $\hat{P}_{(i,j)} = 2(\vec{S}_i \cdot \vec{S}_j + \frac{1}{4})$. All exchange couplings J_a are positive; the signs $(-1)^{n_a}$ are fixed by antisymmetry of the many-body wave function, which implies that exchanges involving an even (odd) number of electrons are antiferromagnetic (ferromagnetic) [27]. The exchange energies J_a can be calculated using the semiclassical instanton method, which is asymptotically exact in the $r_s \rightarrow \infty$ limit:

$$J_a = \hbar\omega_0 \left(\frac{\sqrt{r_s} S_a}{2\pi} \right)^{1/2} A_a \exp[-\sqrt{r_s} S_a]. \quad (3)$$

Here, $\hbar\sqrt{r_s} S_a$ is the classical Euclidean action along the minimal action path that implements the particle exchange labelled by a , S_a is the “dimensionless action,” which is independent of r_s , and $\hbar\omega_0/2 = 1.6274/r_s^{3/2}$ is the zero-point phonon energy (per particle) of the defect-free WC in units of the effective Rydberg energy $\text{Ry} = e^2/8\pi\epsilon a_B$ [15,28]. A_a is the dimensionless fluctuation determinant [29,30], which captures the Gaussian fluctuations around the semiclassical paths, and is generally of order 1. Including all r_s dependencies, $J_a = O(r_s^{-5/4} e^{-\sqrt{r_s} S_a})$. To simplify notation, we often suppress the full indices a in the subscripts of J_a and S_a , and instead label these by n_a —if there are multiple processes involving the same number of particles, we distinguish them with primes (e.g., $S_{4,\text{wc}}$ and $S'_{4,\text{wc}}$, etc.).

In Fig. 1(a), we illustrate the six most important exchange processes for the pure WC and quote the dimensionless actions calculated in Ref. [14]. Although the dimensionless actions for all these processes are quite comparable, the (ferromagnetic) three-particle ring exchange process has the smallest action and hence determines the magnetism in the $r_s \rightarrow \infty$ limit [10–12,14]. The characteristic temperature scale for ferromagnetism, T^* , is set by J_3 ; evaluating Eq. (3) at $r_s \approx 40$ with the parameters of AIs and the fluctuation determinant, $A_3 = 2.19$, calculated in Ref. [14], we find $T^* \sim 0.003$ K. This is 2 orders of magnitude smaller

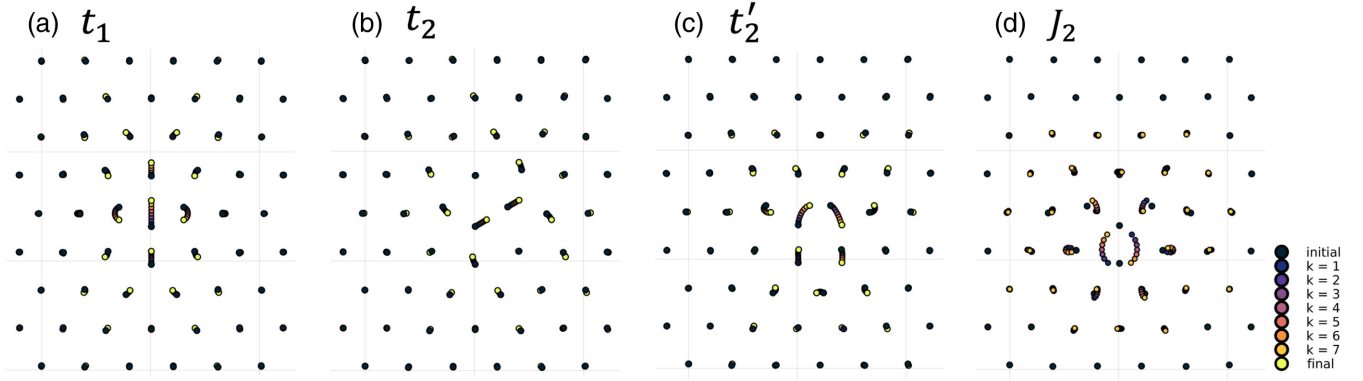


FIG. 2. Visualization of multiparticle tunneling trajectories involving a (relaxed) triangle-centered interstitial: (a)–(c) The three dominant interstitial hopping processes. (d) The most important exchange process involving an interstitial. The corresponding dimensionless actions are (a) $S_{1,\text{hop}} = 0.138$, (b) $S_{2,\text{hop}} = 0.032$, (c) $S'_{2,\text{hop}} = 0.141$, and (d) $S_{2,\text{ex}} = 0.536$, as shown in Fig. 1. The colors indicate seven intermediate configurations, indexed by k , along with the initial and the final configuration.

than the temperature at which the experiments are done ($T \gtrsim 0.3$ K) [5].

In the presence of a triangle-centered interstitial in the WC, new tunneling processes are introduced [Figs. 1(b) and 1(c)]. The semiclassical expression (3) can be used to calculate both exchange interactions involving an interstitial, J_a , and interstitial hopping processes, t_a (where again a labels a particular process). The dimensionless action S_a is calculated numerically by minimizing the Euclidean action $\hbar\sqrt{r_s}S = \int_{\mathbf{X}_i}^{\mathbf{X}_f} dX \sqrt{2m(V - E_0)}$ on a supercell containing $10 \times 12 + 1$ electrons (including the interstitial) with periodic boundary conditions. Here, V is the Coulomb interaction, E_0 is the energy cost of introducing one interstitial in the WC, and \mathbf{X}_i and \mathbf{X}_f are the initial and the final relaxed interstitial configurations, respectively. We discretize the tunneling path to 7 intermediate configurations and allow up to 30 electrons to adjust their positions during the minimization. For exchange processes, all the remaining electrons are fixed at their initial positions, whereas for hopping processes, they move in linearly interpolating paths connecting the initial and the final positions. For minimization, we used the limited-memory Broyden-Fletcher-Goldfarb-Shanno (L-BFGS) algorithm [31]. Coulomb interactions are treated with the standard Ewald method. See Supplemental Material [20] for more details of the calculations.

Figure 1(b) schematically shows various multiparticle exchange processes that involve an interstitial (circled), along with the corresponding dimensionless actions $S_{a,\text{ex}}$. Interstitial hopping processes are shown schematically in Fig. 1(c), along with the dimensionless actions $S_{a,\text{hop}}$. Among these, one cooperative hopping term, t_2 , clearly dominates, as its action, $S_{2,\text{hop}} = 0.032$, is more than an order of magnitude smaller than most others. (Recall that $\sqrt{r_s}S_a$ appears in the exponent of the expressions for J_a or t_a) However, the t_2 term does not connect all the WC sites in the presence of one interstitial, so by itself, it cannot fully

lift the ground state spin degeneracy (see Fig. S2 of the Supplemental Material [20]). The next dominant terms are t_1 and t'_2 [corresponding to $S_{1,\text{hop}}$ and $S'_{2,\text{hop}}$ in Fig. 1(c)]. Together with t_2 , these terms fully determine the magnetism of the WC in the presence of a small density of interstitials. We visualize the tunneling paths corresponding to these three processes, along with one exchange process, in Fig. 2. Keeping these three dominant terms in an effective Hamiltonian:

$$\begin{aligned}
 H_{\text{eff}} = & -t_2 \sum_{\substack{(n,j,n') \\ \in (t_2 \text{ path})}} \sum_{\sigma,\sigma'=\uparrow,\downarrow} c_{n,\sigma}^\dagger f_{j,\sigma}^\dagger f_{j,\sigma'} c_{n',\sigma} \\
 & -t'_2 \sum_{\substack{(n,j,n') \\ \in (t'_2 \text{ path})}} \sum_{\sigma,\sigma'=\uparrow,\downarrow} c_{n,\sigma}^\dagger f_{j,\sigma}^\dagger f_{j,\sigma'} c_{n',\sigma} \\
 & -t_1 \sum_{\langle n,n' \rangle} \sum_{\sigma=\uparrow,\downarrow} c_{n,\sigma}^\dagger c_{n',\sigma} + [U = \infty]. \quad (4)
 \end{aligned}$$

Here, $f_{j\sigma}^\dagger$ is the creation operator of localized electrons that live on the triangular lattice sites j , and $c_{n,\sigma}^\dagger$ is the creation operator of itinerant electrons that live on the triangular plaquette centers n . The last $U = \infty$ condition precludes any doubly occupied sites. One can check explicitly that all these t_a 's are positive.

The remaining tunneling terms that we have omitted from H_{eff} , including the exchange terms J_a , are exponentially smaller than those we have kept. We have also omitted direct (elastic) interactions between interstitials which are small only in proportion to powers of $1/r_s$. These are negligible both because we are interested in the situation with a dilute concentration of interstitials, and because they turn out to be small in the experimentally relevant range of r_s [32].

A single interstitial.—In the presence of one interstitial in the WC, we prove the following theorem—reminiscent of

the proof of Nagaoka ferromagnetism in the $U = \infty$ Hubbard model—using the Perron-Frobenius theorem [27,33,34]:

Theorem.—The ground state of H_{eff} in any finite system in the presence of a single interstitial (i.e., for $\nu = N^{-1} \sum_{j,\sigma} f_{j,\sigma}^\dagger f_{j,\sigma} = 1$ and $\sum_{n,\sigma} c_{n,\sigma}^\dagger c_{n,\sigma} = 1$, where N is the number of WC sites j) is the fully polarized ferromagnet; it is unique up to global spin rotations.

Proof.— H_{eff} commutes with the total spin operator \vec{S}_{total} , so its spectrum consists of degenerate multiplets with definite S_{total}^2 . We show that the ground state multiplet has maximal S_{total}^2 . We restrict attention to the sector of Hilbert space with $S_{\text{total}}^z = 0$ for $N + 1$ even and $S_{\text{total}}^z = \frac{1}{2}$ for $N + 1$ odd, since these lowest $|S_{\text{total}}^z|$ sectors contain one representative state from each multiplet. We define basis states

$$|n, \tau, \{\sigma\}\rangle \equiv c_{n,\tau}^\dagger f_{1,\sigma_1}^\dagger \cdots f_{N,\sigma_N}^\dagger |0\rangle, \quad (5)$$

where n is the position of the interstitial electron, τ is its spin, and the σ_j 's specify the spins of the WC sites, which we number in an arbitrary manner from $j = 1$ to N . All the basis states in Eq. (5) can be reached from any starting state by repeated application of the hopping operators in H_{eff} [Eq. (4)]—we say that the hoppings satisfy the “connectivity condition” [35].

We now consider matrix elements of H_{eff} in this basis: It is easy to see that any state that has a nonzero matrix element with $|n, \tau, \{\sigma\}\rangle$ must be of the form

$$|n', \sigma_j, \{\sigma_1, \dots, \sigma_{j-1}, \tau, \sigma_{j+1}, \dots, \sigma_N\}\rangle \quad \text{or} \quad |n', \tau, \{\sigma\}\rangle.$$

Moreover, it is a simple algebra to show that

$$\begin{aligned} \langle n', \sigma_j, \{\sigma_1, \dots, \sigma_{j-1}, \tau, \sigma_{j+1}, \dots, \sigma_N\} | H_{\text{eff}} | n, \tau, \{\sigma\} \rangle \\ = -t_2 \quad \text{or} \quad -t'_2, \end{aligned} \quad (6)$$

and

$$\langle n', \tau, \{\sigma\} | H_{\text{eff}} | n, \tau, \{\sigma\} \rangle = -t_1, \quad (7)$$

depending on which of the three hopping terms connect the two states. Since H_{eff} satisfies the connectivity condition and all matrix elements are nonpositive, the Perron-Frobenius theorem implies that the ground state is unique and is a superposition of all the basis states $|n, \tau, \{\sigma\}\rangle$ with positive coefficients. This state is necessarily a maximal spin state, i.e., has total spin $S_{\text{total}} = (N + 1)/2$. ■

Note that, in the $S_{\text{total}}^z = (N + 1)/2$ sector, H_{eff} is a noninteracting Hamiltonian, whose ground state is the state where the interstitial electron is in a Bloch state with $\vec{k} = \vec{0}$; the state we have found in the minimal $|S_{\text{total}}^z|$ sector is thus related to this state by repeated applications of the global spin-lowering operator.

Phase diagram.—Although the exchange terms omitted in Eq. (4) are exponentially smaller than those we have kept, the former terms can be important when considering the thermodynamic limit, $N \rightarrow \infty$. In particular, whenever the bulk exchange couplings J_a favor anything other than the ferromagnetic state, a single interstitial can only polarize a finite number of WC sites to become a ferromagnetic polaron [36]. (Note that a Monte Carlo study found that for the pure WC, antiferromagnetic correlations are favored for $r_s \lesssim 175$ [13].) The size of the ferromagnetic polaron is determined by the competition between the energy gain to delocalize the interstitial within a region of radius R , $t \cdot (a/R)^2$, and the energy cost, $J \cdot (R/a)^2$, to destroy the antiferromagnetism there, where J is an appropriate sum of the microscopic antiferromagnetic exchange interactions, and a is a lattice constant of the WC. Minimizing the free energy, we obtain the size of the ferromagnetic polaron:

$$R_{\text{polar}}^2 \sim a^2 \sqrt{t/J} \sim a^2 \exp\left(\frac{1}{2} \sqrt{r_s} \alpha_{\text{polar}}\right), \quad (8)$$

where t is an appropriate sum of t_2 , t'_2 , and t_1 . (When $t > T > J$, J is substituted by T in the estimate of the polaron size.) By comparing the results for J_a and t_a summarized in Fig. 1, it is to be expected that $\alpha_{\text{polar}} \approx 1$.

The properties of H_{eff} with a finite filling of interstitials, $\nu_{\text{int}} > 0$, are nontrivial, and the complexity is increased if we include the effect of antiferromagnetic interactions, $J > 0$. However, for $t/J \gg 1$, certain general features of the phase diagram can be inferred by analogy with the behavior of the ordinary Hubbard model at large U/t in the presence of a dilute concentration of holes [19,36–39]: It is likely that at $T = 0$, for a range of dopings $\nu_{\text{int}} \in (0, \nu_c)$, there is two-phase coexistence between an insulating antiferromagnetic phase and a half-metallic ferromagnetic phase, with $\nu_c \sim a^2/R_{\text{polar}}^2$. The fully polarized ferromagnetic phase then likely appears for a range of fillings, $\nu_{\text{int}} > \nu_c$. Furthermore, the temperature scale for the onset of ferromagnetism can be estimated to be proportional to the Fermi energy, $T^* \sim \nu_{\text{int}} \cdot t$.

Quantitative considerations in AIs.—To flesh out the general discussion, we evaluate various quantities with the parameters relevant to AIs ($\epsilon = 10 \epsilon_0$ and $m = 0.46 m_e$, where ϵ_0 is the vacuum permittivity and m_e is the electron mass) in the insulating phase close to the metal-insulator transition, i.e., with $r_s \approx 40$. The zero-point phonon energy in the presence of an interstitial is $\hbar\omega_0/2 = 1.034/r_s^{3/2}$ in units of the effective Rydberg energy, $\text{Ry} = 731 \text{ K}$ [15]. Using the same value for the fluctuation determinant as for J_3 of the pure WC, $A_3 = 2.19$, Eq. (3) gives $t_2 \sim 1.9$, $t'_2 \sim 2$, $t_1 \sim 2 \text{ K}$, and hence $t \sim t_2 + t'_2 + t_1 \sim 6 \text{ K}$, a much higher energy scale than that of the pure WC for which $J \sim 0.003 \text{ K}$. (The latter is in the same ballpark as estimates of J from the path integral Monte Carlo

calculation [13].) This means that for $\nu_{\text{int}} \approx \nu_c$, the temperature scale for ferromagnetism is $T^* \sim \sqrt{Jt} \sim 0.1$ K.

Phenomenological considerations.—While our calculations show that an interstitial in a WC generates a large ferromagnetic polaron, the relevance of this observation to any experimental system turns on other considerations. The existence of a finite concentration of interstitials is surely not a universal feature of a WC phase; in any scenario we have analyzed, their density is found to depend on assumed microscopic details.

Let us first consider the scenario in which a small density of interstitials is introduced from nearby coexisting (higher-density) Fermi-liquid (FL) regions, as discussed earlier. If the interstitial density is sufficiently large, and if the WC regions percolate throughout the sample, it can result in a ferromagnetic phase in which the WC regions are fully polarized. Given that the FL at large r_s has a large ferromagnetic susceptibility, it is also possible to imagine circumstances in which the FL puddles, as well, are driven ferromagnetic by their interactions with the ferromagnetic WC. We propose that such a picture may apply to the fully polarized insulating phase found in AIs quantum wells [5].

We can also imagine cases in which interstitials are induced by extrinsic sources even in the absence of FL regions: e.g., due to a slowly varying disorder potential and/or a weak commensurate locking of the WC to the potential from the underlying semiconductor (especially when this period is large, as in a Moiré system). We note that, in contrast to the AIs system, a fully polarized insulating phase is not observed in a recent experiment on another 2DEG in a MgZnO/ZnO heterostructure [40]. What material-specific aspect of these systems is responsible for this dichotomy is presently unclear. These are all issues we hope to address in future work.

We thank Boris Spivak for initial insights which led to this investigation. We also thank Peter Littlewood, Eun-Ah Kim, Ilya Esterlis, Mansour Shayegan, Brian Skinner, Inti Sodemann, and Joseph Falson for helpful comments on the draft. This work was supported in part by NSF Grant No. DMR-2000987 at Stanford (K.-S. K. and S. A. K.), the Gordon and Betty Moore Foundation's EPiQS Initiative through GBMF8686 (C.M.), and the Stanford Graduate Fellowship (A.P.). Parts of the computing for this project were performed on the Sherlock computing cluster at Stanford University.

*Corresponding author.
kyungsu@stanford.edu

- [1] E. Wigner, On the interaction of electrons in metals, *Phys. Rev.* **46**, 1002 (1934).
[2] B. Tanatar and D. M. Ceperley, Ground state of the two-dimensional electron gas, *Phys. Rev. B* **39**, 5005 (1989).

- [3] N. D. Drummond and R. J. Needs, Phase Diagram of the Low-Density Two-Dimensional Homogeneous Electron Gas, *Phys. Rev. Lett.* **102**, 126402 (2009).
[4] C. Attacalite, S. Moroni, P. Gori-Giorgi, and G. B. Bachelet, Correlation Energy and Spin Polarization in the 2D Electron Gas, *Phys. Rev. Lett.* **88**, 256601 (2002).
[5] M. S. Hossain, M. Ma, K. V. Rosales, Y. Chung, L. Pfeiffer, K. West, K. Baldwin, and M. Shayegan, Observation of spontaneous ferromagnetism in a two-dimensional electron system, *Proc. Natl. Acad. Sci. U.S.A.* **117**, 32244 (2020).
[6] M. S. Hossain, M. K. Ma, K. A. Villegas-Rosales, Y. J. Chung, L. N. Pfeiffer, K. W. West, K. W. Baldwin, and M. Shayegan, Spontaneous Valley Polarization of Itinerant Electrons, *Phys. Rev. Lett.* **127**, 116601 (2021).
[7] K.-S. Kim and S. A. Kivelson, Discovery of an insulating ferromagnetic phase of electrons in two dimensions, *Proc. Natl. Acad. Sci. U.S.A.* **118**, e2023964118 (2021).
[8] S. A. Vitkalov, H. Zheng, K. M. Mertes, M. P. Sarachik, and T. M. Klapwijk, Scaling of the Magnetoconductivity of Silicon MOSFETs: Evidence for a Quantum Phase Transition in Two Dimensions, *Phys. Rev. Lett.* **87**, 086401 (2001).
[9] A. A. Shashkin, S. V. Kravchenko, V. T. Dolgoplov, and T. M. Klapwijk, Indication of the Ferromagnetic Instability in a Dilute Two-Dimensional Electron System, *Phys. Rev. Lett.* **87**, 086801 (2001).
[10] M. Roger, Multiple exchange in ^3He and in the Wigner solid, *Phys. Rev. B* **30**, 6432 (1984).
[11] S. Chakravarty, S. Kivelson, C. Nayak, and K. Voelker, Wigner glass, spin liquids and the metal-insulator transition, *Philos. Mag. B* **79**, 859 (1999).
[12] M. Katano and D. S. Hirashima, Multiple-spin exchange in a two-dimensional Wigner crystal, *Phys. Rev. B* **62**, 2573 (2000).
[13] B. Bernu, L. Cândido, and D. M. Ceperley, Exchange Frequencies in the 2D Wigner Crystal, *Phys. Rev. Lett.* **86**, 870 (2001).
[14] K. Voelker and S. Chakravarty, Multiparticle ring exchange in the Wigner glass and its possible relevance to strongly interacting two-dimensional electron systems in the presence of disorder, *Phys. Rev. B* **64**, 235125 (2001).
[15] E. Cockayne and V. Elser, Energetics of point defects in the two-dimensional Wigner crystal, *Phys. Rev. B* **43**, 623 (1991).
[16] D. S. Fisher, B. I. Halperin, and R. Morf, Defects in the two-dimensional electron solid and implications for melting, *Phys. Rev. B* **20**, 4692 (1979).
[17] L. Cândido, P. Phillips, and D. M. Ceperley, Single and Paired Point Defects in a 2D Wigner Crystal, *Phys. Rev. Lett.* **86**, 492 (2001).
[18] A. Meierovich and B. Spivak, Quantum magnetic-properties of the interface between solid and liquid ^3He , *JETP Lett.* **34**, 551 (1981), http://jetpletters.ru/ps/1535/article_23484.pdf.
[19] B. Spivak and F. Zhou, Ferromagnetic correlations in quasi-one-dimensional conducting channels, *Phys. Rev. B* **61**, 16730 (2000).
[20] See Supplemental Material at <http://link.aps.org/supplemental/10.1103/PhysRevLett.129.227202> for the details of the numerical calculation of the semiclassical actions.

- [21] Y. Imry and M. Wortis, Influence of quenched impurities on first-order phase transitions, *Phys. Rev. B* **19**, 3580 (1979).
- [22] M. Aizenman and J. Wehr, Rounding of First-Order Phase Transitions in Systems with Quenched Disorder, *Phys. Rev. Lett.* **62**, 2503 (1989).
- [23] B. Spivak, Phase separation in the two-dimensional electron liquid in MOSFET's, *Phys. Rev. B* **67**, 125205 (2003).
- [24] B. Spivak and S. A. Kivelson, Phases intermediate between a two-dimensional electron liquid and Wigner crystal, *Phys. Rev. B* **70**, 155114 (2004).
- [25] R. Jamei, S. Kivelson, and B. Spivak, Universal Aspects of Coulomb-Frustrated Phase Separation, *Phys. Rev. Lett.* **94**, 056805 (2005).
- [26] B. Spivak and S. A. Kivelson, Transport in two dimensional electronic micro-emulsions, *Ann. Phys. (Amsterdam)* **321**, 2071 (2006).
- [27] D. Thouless, Exchange in solid ^3He and the Heisenberg Hamiltonian, *Proc. Phys. Soc. London* **86**, 893 (1965).
- [28] L. Bonsall and A. Maradudin, Some static and dynamical properties of a two-dimensional Wigner crystal, *Phys. Rev. B* **15**, 1959 (1977).
- [29] A. Altland and B. D. Simons, *Condensed Matter Field Theory* (Cambridge University Press, Cambridge, England, 2010).
- [30] S. Coleman, *Aspects of Symmetry: Selected Erice Lectures* (Cambridge University Press, Cambridge, England, 1988).
- [31] P. K. Mogensen and A. N. Riseth, Optim: A mathematical optimization package for Julia, *J. Open Source Software* **3**, 615 (2018).
- [32] The elastic interactions are expected to scale as $O(r_s^{-3})$ [16], so they are indeed large in the strict asymptotic sense compared to any tunneling term. However, the very small value of, for example, $S_{2,\text{hop}}$ means that even for quite large r_s , the exponential factor is not dominant, e.g., $\exp(-\sqrt{r_s}S_{2,\text{hop}}) = 0.64$ at $r_s = 200$. Thus, the fact that the prefactor of the tunneling terms is $O(r_s^{-5/4})$ means that those with small action tend to be larger than the elastic interactions in the experimentally relevant range of r_s .
- [33] Y. Nagaoka, Ferromagnetism in a narrow, almost half-filled s band, *Phys. Rev.* **147**, 392 (1966).
- [34] H. Tasaki, Extension of Nagaoka's theorem on the large- U Hubbard model, *Phys. Rev. B* **40**, 9192 (1989).
- [35] That the connectivity condition is satisfied can be seen as follows: The t_2 (or t'_2) processes exchange the spin of the interstitial with that of a neighboring WC site, while t_1 processes simply move the interstitial around. By composing these, we can arbitrarily permute the spins of the WC.
- [36] D. P. Arovas, E. Berg, S. A. Kivelson, and S. Raghu, The Hubbard model, *Annu. Rev. Condens. Matter Phys.* **13**, 239 (2022).
- [37] V. J. Emery, S. A. Kivelson, and H. Q. Lin, Phase Separation in the $t - J$ Model, *Phys. Rev. Lett.* **64**, 475 (1990).
- [38] E. Eisenberg, R. Berkovits, D. A. Huse, and B. L. Altshuler, Breakdown of the Nagaoka phase in the two-dimensional $t - J$ model, *Phys. Rev. B* **65**, 134437 (2002).
- [39] L. Liu, H. Yao, E. Berg, S. R. White, and S. A. Kivelson, Phases of the Infinite U Hubbard Model on Square Lattices, *Phys. Rev. Lett.* **108**, 126406 (2012).
- [40] J. Falson, I. Sodemann, B. Skinner, D. Tabrea, Y. Kozuka, A. Tsukazaki, M. Kawasaki, K. von Klitzing, and J. H. Smet, Competing correlated states around the zero-field Wigner crystallization transition of electrons in two dimensions, *Nat. Mater.* **21**, 311 (2022).